Journal of the European Ceramic Society **11** (1993) 407–415

Effect of Excess of Iron Oxide and Lead Oxide on the Microstructure and Dielectric Properties of Lead–Iron Tungstate Ceramics

P. M. Vilarinho & J. L. Baptista

Departamento de Engenharia Cerâmica e do Vidro/INESC, Universidade de Aveiro, 3800 Aveiro, Portugal

(Received 7 July 1992; revised version received 4 August 1992; accepted 30 September 1992)

Abstract

Lead–iron tungstate ($Pb(Fe_{2/3}W_{1/3})O_3$; PFW) perovskite ceramics were prepared by the conventional mixed oxides method. Additional amounts of Fe_2O_3 and PbO were used to examine the role of excess oxides on the phase development, densification behaviour and dielectric properties. The stoichiometric mixture of the oxides results in a residual phase (Pb_2WO_5) besides the perovskite. Excess Fe_2O_3 eliminates the Pb_2WO_5, with a marked increase in the dielectric constant, whereas excess PbO leads to an unexpected increase of the amount of the second phase and a consequent decrease of the dielectric constant. The densification behaviour and the microstructures obtained after firing were very dependent on the starting stoichiometry. The PFW phase obtained using PbO or Fe_2O_3 excesses shows various degrees of ordering which seem to be correlated with the presence of either W^{6+} vacancies or of Pb^{2+} vacancies.

$Pb(Fe_{2/3}W_{1/3})O_3$-Keramiken (PFW) mit Perovskit-Struktur wurden auf konventionellem Wege aus Oxidmischungen hergestellt. Um den Einfluß überschüssiger Oxidanteile auf die Phasenbildung, das Verdichtungsverhalten und die dielektrischen Eigenschaften zu untersuchen, wurden auch Zusammensetzungen mit zusätzlichen Anteilen an Fe_2O_3 und PbO hergestellt. Stöchiometrische Mischungen der Oxide führen zur Bildung der Phase Pb_2WO_5 neben dem Perovskit. Bei zusätzlich zugegebenem Fe_2O_3 kann diese Phase vermieden werden, was sich durch einen deutlichen Anstieg der Dielektrizitätskonstanten äußert. Der Zusatz von PbO dagegen ergibt eine unerwartete Zunahme des Anteils der sekundären Phase und führt dementsprechend zu einer Abnahme der Dielektrizitätskonstanten. Das Verdichtungsverhalten und das Gefüge der gebrannten Keramik hängen im starkem Maße von der Ausgangszusammensetzung ab. Die PFW-Phase, die mit PbO- oder Fe_2O_3-Überschuß hergestellt wurde, zeigt verschiedene Ordnungsgrade. Diese Beobachtung scheint mit der Präsenz von W^{6+}-oder Pb^{2+}-Leerstellen verknüpft zu sein.

Des céramiques du tungstate mixte plomb–fer, de forme perovskite ($Pb(Fe_{2/3}W_{1/3})O_3$; PFW), ont été préparées par la méthode classique du mélange des oxydes. Par l'addition supplémentaire de Fe_2O_3 et de PbO, on a pu examiner le rôle des oxydes en excès sur le développement des phases, le comportement à la densification et les propriétés diélectriques. Le d'oxydes stoechiométrique conduit à la formation d'une phase résiduelle (Pb_2WO_5), en plus de la perovskite. Un excès de Fe_2O_3 permet d'éliminer Pb_2WO_5, avec une augmentation sensible de la constante diélectrique, tandis qu'un excès de PbO conduit à une augmentation inattendue de la phase secondaire et en conséquence résulte en une diminution de la constante diélectrique. La densification et les microstructures obtenues après cuisson sont aussi très dépendantes de la stoechiométrie de départ. La phase PFW présente divers degrés d'ordre selon l'excès en PbO ou Fe_2O_3, ce que les auteurs corrèlent avec la présence tantôt de lacunes en W^{6+}, tantôt de lacunes en Pb^{2+}.

1 Introduction

Lead–iron tungstate ($Pb(Fe_{2/3}W_{1/3})O_3$; PFW), is a ferroelectric material, with a diffuse phase transition at approximately 185 K[1]. It was suggested[2] that its disordered perovskite-type structure, in which the Fe^{3+} and W^{6+} ions are randomly distributed in octahedral positions, gives rise to compositional

In part presented at the 2nd Conference of the European Ceramic Society, Augsburg, Germany, September 1991.

Journal of the European Ceramic Society 0955-2219/93/$6.00

fluctuations and a distribution of Curie points in the material, responsible for the diffuse transition. PFW has also a relaxor-type behaviour. A polar glass model for the lead–magnesium niobate (PMN) rhombohedral family of relaxors has been recently suggested,[3] with thermally activated polarization fluctuations occurring between nano- or micropolar regions[4] above a static freezing temperature, but below the ferroelectric paraelectric phase transition.

Like many other perovskites, PFW has been used to obtain solid solutions with dielectric parameters adjusted to make multilayer ceramic capacitors, meeting appropriate standard specifications. Its low Transition Temperature value adjusts the dielectric maximum to room temperature, in systems like

$Pb(Fe_{2/3}W_{1/3})O_3$–$Pb(Mg_{1/3}Ta_{2/3})O_3$,[5]
$Pb(Fe_{2/3}W_{1/3})O_3$–$Pb(Mg_{1/2}W_{1/2})O_3$,[6]
$Pb(Fe_{2/3}W_{1/3})O_3$–$Pb(Fe_{1/2}Nb_{1/2})O_3$,[7-10]
$Pb(Fe_{2/3}W_{1/3})O_3$–$Pb(Fe_{1/2}Nb_{1/2})O_3$
–$Pb(Zn_{1/3}Nb_{2/3})O_3$.[11-13]

Some of these are reported in recent patents[14-16] and are commercial relaxor-based compositions.

It is well known that monophasic perovskite relaxors are difficult to obtain; the appearance of stable second phases, normally of lower permittivity, damages the final electrical properties. Different methodologies have been used to maximize the perovskite phase, including the repeated calcination for long periods of time,[17] corrections in the sintering cycle,[18] the prereaction of B-site oxides to form the columbite-type structure compound ($B'B''_2O_6$) in the systems $Pb(B'_{1/3}B''_{2/3})O_3$,[19] or to form the wolframite-type structure compound ($B'B''O_4$) in the systems $Pb(B'_{1/2}B''_{1/2})O_3$,[20] and the additions of excess oxides.[21-26]

The effect of excess PbO and MgO in the production and properties of $Pb(Mg_{1/3}Nb_{2/3})O_3$ (PMN) has been frequently studied. In the reported results there is general agreement about the role of the excess MgO.[21-24] On the other hand, the studies using excess PbO[18,23-26] lead to different results, some of them quite contradictory.[18,23] However, every reported result shows that PMN ceramics with excess PbO present a high density, achieved by liquid-phase sintering,[18,23-26], although increases[18,25] and decreases[24,26] of dielectric constant have been reported and attributed to microstructure differences, resulting either from different processing conditions or from the different purity of the raw materials.[24,27]

To the authors' knowledge no such detailed work, concerning variations in stoichiometry, has been undertaken for PFW.

In the present work additional amounts of Fe_2O_3 and PbO were used to examine the role of excess oxides in the synthesis of PFW, in its densification behaviour and in the microstructure obtained by the sintering process, trying to correlate these features with the final dielectric properties. Results of X-ray diffraction, scanning electron microscopy, energy dispersive spectroscopy analysis and dielectric measurements will be presented and discussed.

2 Experimental

Reagent grade oxides of lead, iron and tungsten were used to prepare, by conventional mixed oxides processing, the compositions indicated in Table 1. Appropriate proportions of the powders were ball-milled in ethanol for 4 h using agate mills and balls. The reactions taking place on heating the mixtures were identified by thermal analysis (DTA) using an heating rate of 5°C min^{-1}. The compounds formed were identified by X-ray analysis of samples calcined for 2·5 h at temperatures slightly above the exo- or endothermic effects observed.

The results of the thermal analysis lead to a standardized method of sample preparation for ceramic processing. After ball milling the powders for 4 h in ethanol, they were dried at 100°C for several hours and calcined at 780°C for 2·5 h, ground in an agate mortar and remilled, for 8–10 h, to obtain powders of less than 5 μm of particle size. Pellets of 10 mm of diameter and 2–3 mm of thickness were uniaxially pressed at about 127 MPa and then isostatically pressed at about 250 MPa in order to get green densities of 6 g cm^{-3} (PFW Theoretical density = 8·6 g cm^{-3}).[28] An isothermal sintering was performed at 880°C for 2 h.

The internal standard X-ray method was used to

Table 1. Compositions of the samples and sintering characteristics of the PFW ceramics (sintered at 880°C/2 h)

Designation	*Compositions oxide excess*	*Weight loss (wt%)*	*Density (g cm^{-3})*	*Grain size (μm)*
PFW	$Pb(Fe_{2/3}W_{1/3})O_3$	0·35	8·6	2·9
PFW2F	$Pb(Fe_{2/3}W_{1/3})O_3$ + 0·02 mol Fe_2O_3	0·41	8·7	3·8
PFW5F	$Pb(Fe_{2/3}W_{1/3})O_3$ + 0·05 mol Fe_2O_3	0·35	8·7	3·1
PFW10F	$Pb(Fe_{2/3}W_{1/3})O_3$ + 0·10 mol Fe_2O_3	0·26	8·7	4·0
PFW2P	$Pb(Fe_{2/3}W_{1/3})O_3$ + 0·02 mol PbO	—	8·6	3·2
PFW5P	$Pb(Fe_{2/3}W_{1/3})O_3$ + 0·05 mol PbO	0·37	8·4	3·0
PFW10P	$Pb(Fe_{2/3}W_{1/3})O_3$ + 0·10 mol PbO	0·64	8·0	2·3

determine the amount of the Pb_2WO_5 phase present in the different calcined samples; NiO was used as a standard. The amounts of Pb_2WO_5 phase in the unknown mixtures were determined from a calibration curve, obtained from known proportions of PFW and Pb_2WO_5.

Routinely the calcined and sintered specimens were examined by X-ray diffraction analysis to identify the phases formed.

The microstructure of the samples were observed in fractured and polished sections using scanning electron microscopy (SEM) with X-ray energy dispersive spectroscopy (EDS), for chemical analysis.

Dielectric constant and dielectric loss were measured at 10, 50 and 100 kHz, as a function of temperature using an Air Product Displex cryostat and a HP4277A LCZ bridge.

3 Results and Discussion

3.1 Synthesis

3.1.1 Stoichiometric proportions of oxides

The DTA curve obtained from the powders mixed in the stoichiometric proportions of PFW (Fig. 1), shows five thermic peaks. From 300 to 600°C two exothermic peaks occur at about 330°C and 550°C, respectively. Between 660 and 750°C two consecutive well-defined peaks are present, an endothermic at about 680°C and an exothermic at about 720°C, and a final endothermic one can be seen at about 900°C.

The samples calcined at 330, 550, 690, 725 and 870°C have been analysed by X-ray diffraction (Fig. 2). The reaction between lead oxide and tungsten oxide gave rise to the formation of two lead tungstate phases, $PbWO_4$ and Pb_2WO_5, corresponding to the first exothermic peaks (330 and 550°C). Yonezawa & Ohno[29] and Lu *et al.*[30] have also reported the sequential formation of $PbWO_4$ and Pb_2WO_5, while Kassarjian *et al.*[11] reported only the formation of $PbWO_4$ at 350°C.

At a temperature of about 690°C the Pb_2WO_5

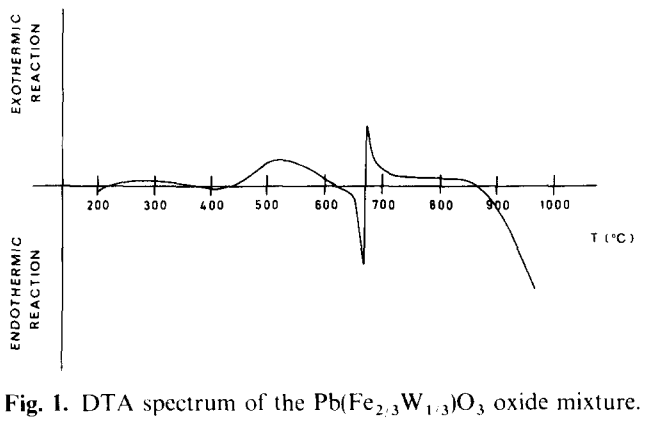

Fig. 1. DTA spectrum of the $Pb(Fe_{2/3}W_{1/3})O_3$ oxide mixture.

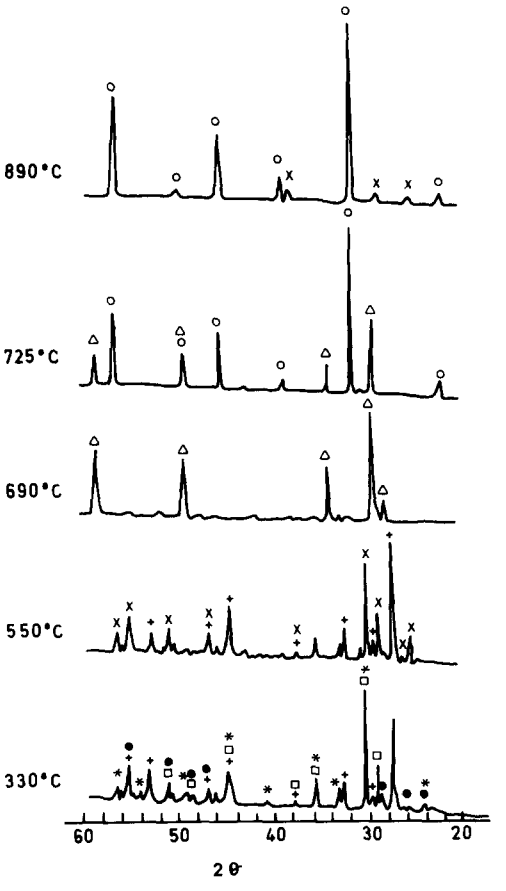

Fig. 2. X-Ray diffractograms of $Pb(Fe_{2/3}W_{1/3})O_3$ oxide mixture calcined at 330, 550, 690, 725 and 890°C. ○, PFW; △, pyrochlore; ×, Pb_2WO_5; +, $PbWO_4$; ●, WO_3; ★, Fe_2O_3; □, PbO.

compound disappeared and a pyrochlore-type phase was formed, by reaction of the lead tungstates with Fe_2O_3. In agreement with these results, the formation of the pyrochlore-type phase is reported in all works, as occurring at temperatures higher than 670°C and is attributed to the reaction between the lead tungstate phases and iron oxide (endothermic reaction). Lu *et al.*[30] suggested that the endothermic peak (690°C) is due to the formation of a liquid, from an intermediate unknown solid phase, and that the pyrochlore phase is formed from this liquid. The chemical composition of the pyrochlore phase is referred to as being $Pb_2Fe_{2/3}W_{4/3}O_7$ by Agranovskaya;[1] however, Lu *et al.*[30] reported that the pyrochlore phase had the ratio Pb:Fe:W = 2:1:1.

As can be seen in X-ray diffractograms (Fig. 2) the pyrochlore phase converts to the perovskite $Pb(Fe_{2/3}W_{1/3})O_3$ above 720°C (exothermic reaction), but peaks corresponding to Pb_2WO_5 could again be detected. The published results[1,11,13,29,30] refer also to the formation of the perovskite phase PFW for temperatures above 700°C. Lu *et al.*[31] report that, in spite of several efforts to obtain PFW single-phase material, trace amounts of Pb_2WO_5 were not eliminated. The same authors attempted to prepare by solid-state reaction and coprecipitation the $Pb_2FeWO_{6.5}$ pyrochlore phase.[32] The product

Table 2. The amount of Pb_2WO_5 phase determined by the internal standard X-ray method

Compositions	*Pb_2WO_5 (%)*
PFW	14
PFW2F	4
PFW5F	—
PFW10F	—
PFW2P	25
PFW5P	29
PFW10P	34

they obtained was stable below 700°C and, above this temperature, decomposed to $Pb(Fe_{2/3}W_{1/3})O_3$ and $PbWO_4$. The melting of the PFW phase occurs for temperatures above 900°C.[33]

3.1.2 Excess of Fe_2O_3 and PbO

The DTA curves for the different compositions with iron and lead oxide excess (Table 1) are similar to the one already presented (Fig. 1).

To study the influence of the excess of iron and lead oxide on the relative proportions of the phases formed, the calcined samples were analysed by the internal standard X-ray method. The results are summarized in Table 2. It can be seen that the amount of Pb_2WO_5 is reduced by the addition of excess Fe_2O_3, being undetectable by X-ray diffraction for the PFW5F and PFW10F compositions. The addition of excess PbO, quite unexpectedly, raises the amount of the lead tungstate phase.

3.2 Sintering

Table 1 summarizes the sintering characteristics: weight loss, density and average grain size of all compositions, sintered at 880°C for 2 h. All the compositions attained a high degree of densification with small weight losses.

3.2.1 Stoichiometric proportions of the oxides

The fractured surfaces of PFW show an intergranular fracture, a dense matrix and sometimes vestiges of a liquid surrounding the grains (Fig. 3(a)). From the polished and thermally etched surface the presence of a second phase between the matrix grains can be detected. This phase presents an elongated shape, and has a 'molten' aspect (Fig. 3(b)). EDS analysis revealed that this phase is rich in Pb and W, allowing its identification with the Pb_2WO_5 phase detected by X-ray diffraction.

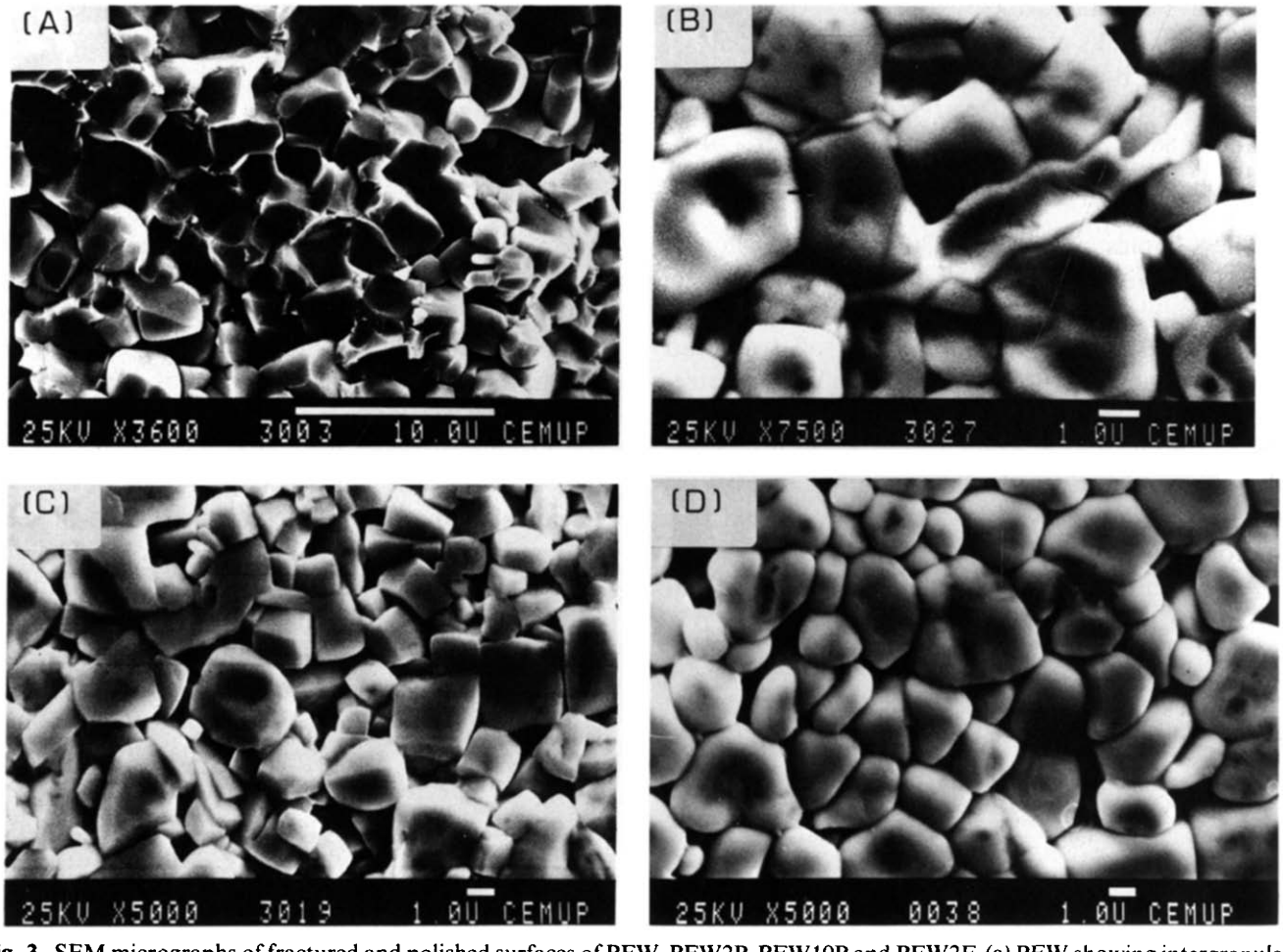

Fig. 3. SEM micrographs of fractured and polished surfaces of PFW, PFW2P, PFW10P and PFW2F. (a) PFW showing intergranular fracture and the presence of the liquid phase surrounding the grains. (b) PFW2P showing the 'molten' aspect of the second phase (Pb_2WO_5). (c) PFW10P and (d) PFW2F showing the more porous microstructure and the polyhedrally shaped grains of PbO excess sample, compared with the denser microstructure and rounded grains of the Fe_2O_3 excess sample.

3.2.2 Excess of Fe_2O_3 and PbO

Table 1 shows that the excess iron samples present a high degree of densification, and a slight increase in grain size, by comparison with the stoichiometric PFW compositions. On the other hand, the excess lead samples exhibit a tendency to lower values of fired density and smaller grain sizes.

The presence of the second phase, with a 'molten' aspect, between the matrix grains became more important for the compositions with excess lead oxide, in agreement with the increased amount of Pb_2WO_5 detected by X-ray diffraction (Fig. 3(b)). The lead oxide excess samples also reveal a more porous microstructure with polyhedrally shaped grains (Fig. 3(c)).

Compositions with iron oxide excess show a dense microstructure, similar to that of PFW, with rounded grains (Fig. 3(b)). It was not possible to detect the molten phase on the microstructure of the samples with 0·05 and 0·10 mol excess Fe_2O_3. For the composition PFW5F and PFW10F, groups of small grains were detected on the corners of some of the matrix grains (Fig. 4). Iron was the only element detected by EDS in the small grains. Iron oxide was detected by X-ray diffraction.

Constant heating rate dilatometry (CHR) was used to study the sintering behaviour of selected samples. CHR dilatometry derivative curves for the compositions PFW, PFW10F and PFW10P are presented in Fig. 5. It can be seen that the curves of PFW and PFW10F have similar behaviour, which is quite different from that of PFW10P. While the former show a continuous increase in the shrinkage rate up to about 880°C, the PFW10P curve, after a rapid increase of the shrinkage rate between 630 and 715°C, present a marked reduction of this parameter. A rapid increase in the shrinkage rate occurs from 890°C upwards, as in the two other curves.

In the relaxor niobate systems[18,23–26] excess PbO tends to promote densification by liquid-phase sintering. The results of Fig. 5 show that the tungstate relaxor has a different behaviour. The shrinkage peak at about 700°C, in the sample with excess PbO, is most probably due to the Pb_2WO_5 phase. The 'molten' aspect of this phase suggests however that it is present as a 'viscous' liquid. The presence of a liquid can accelerate the densification process, either by enhancement of the matter transport within a reactive liquid phase, or by a process of rearrangement caused by the sliding of the grains. For this particular case, the presence of a 'molten' phase between the matrix grains and the polyhedral shape of the grains, whose shape and size seem to be little altered by the sintering process, suggests that the most probable mechanism is that of rearrangement. It is known that this process can lead to up to 15% of shrinkage.[34]

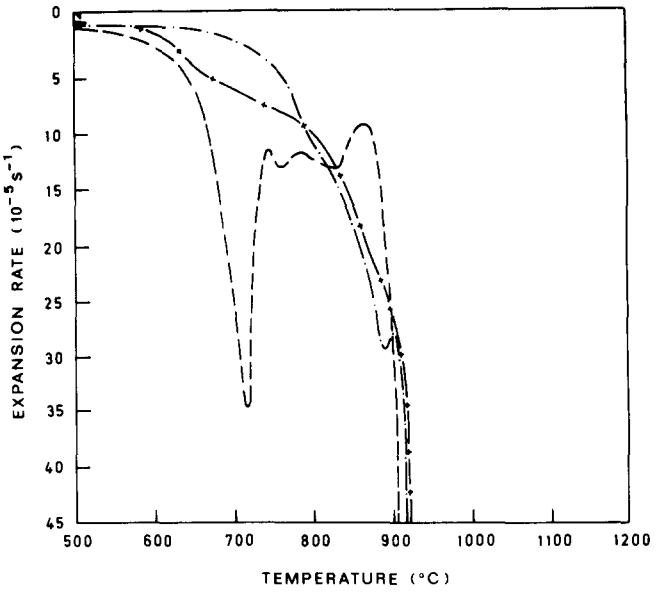

Fig. 5. Derivative curve of CHR dilatometry (heating rate 10°C min^{-1}) of (– + – + –) PFW, (—·—·—) PFW10F (PFW + 0·10 mol Fe_2O_3) and (— – —) PFW10P (PFW + 0·10 mol PbO).

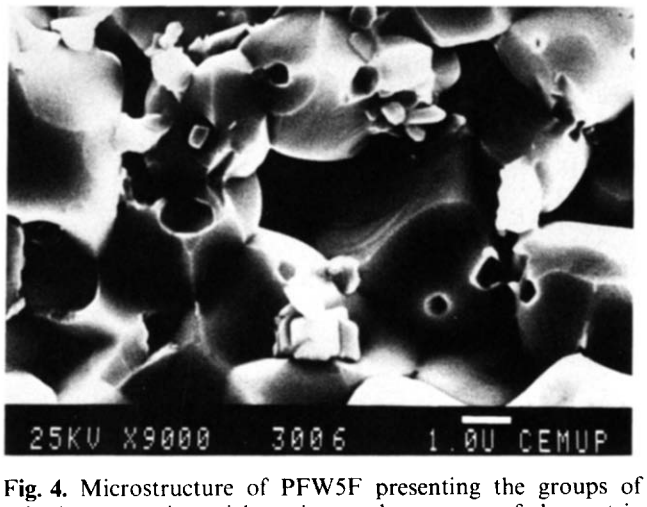

Fig. 4. Microstructure of PFW5F presenting the groups of submicrometer iron-rich grains at the corners of the matrix grains.

In contrast, for samples with excess Fe_2O_3, the gradual increase of the shrinkage rate (PFW10F curve) observed up to 880°C, is more typical of a sintering process dominated only by a matter transport mechanism[35,36] until appreciable grain growth occurs. The matter transport between areas of different chemical potential, at the surfaces of particles, leads to the rounding of the grains simultaneously with the densification, as can be observed in Fig. 3(d). This observation corroborates the pronounced effect of matter transport in this system, when compared to the other one.

The appearance of a liquid phase in the PFW system, at temperatures near 900°C, has been reported before[33] and is responsible for the sudden rise of the shrinkage rate (Fig. 5), in both systems, as well as for the marked deformation of the sample above this temperature.

In the sample with lead oxide excess isothermally sintered some porosity persists (Fig. 3(c)). This difficulty in removing the final porosity could be related to (i) the decrease of matter transport by diffusion when compared with the other systems (for the samples with PbO excess the initial shrinkage rate is at 716°C higher ($3{\cdot}5 \times 10^{-4}\,s^{-1}$) than that observed in the excess iron system ($1{\cdot}8 \times 10^{-5}\,s^{-1}$); however for higher temperatures (>880°C) this situation is inverted; the shrinkage rate is, for the excess lead oxide system, about $1{\cdot}5 \times 10^{-4}\,s^{-1}$, while it has a value of $3{\cdot}0 \times 10^{-4}\,s^{-1}$, almost double, for the excess iron oxide system), or (ii) by the presence of sintering tensions originating during the sintering of two different phases (matrix of PFW and Pb_2WO_5).

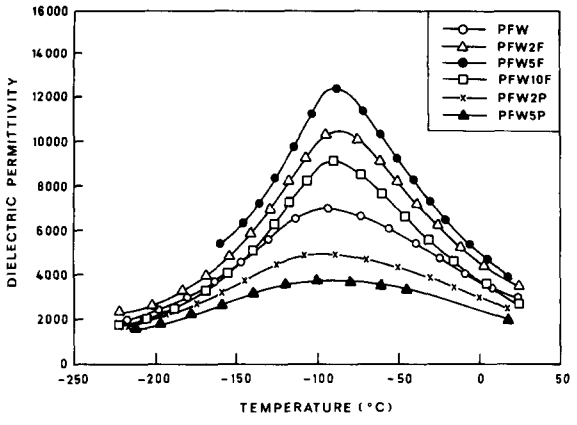

Fig. 6. The effect of excess Fe_2O_3 and PbO on the dielectric constant of PFW ceramics, as a function of temperature, at 10 kHz.

3.3 Dielectric properties

The dielectric characteristics of PFW and the effects of excess Fe_2O_3 and PbO on the dielectric properties are shown in Fig. 6 and Table 3.

The diffuseness (δ) of the transition, which characterizes the breadth of the transition peak, was calculated for all compositions, using the Gaussian distribution relation[37]

$$E_{rmax} = E_r \exp[(T - T_0)^2/2\delta_g^2]$$

where E_{rmax} is the maximum relative dielectric constant, E_r the relative dielectric constant, T_0 the temperature at which E_{rmax} occurs and δ_g the Gaussian diffuseness. A method of limiting the temperature range to that corresponding to 2/3 of the maximum relative dielectric constant was used.[37] This limitation allowed consistent and representative diffuseness values to be obtained, without taking into account contributions arising from different temperature ranges of measurements, or from the relaxor behaviour of the material.

For the samples with iron oxide excess, the maximum of the dielectric constant increases, reaching 12300 for PFW5F, and dropping afterwards to 9000 for PFW10F (Fig. 7(a)). The temperature of the ferroelectric paraelectric transition (T_0), measured at 10 kHz, varies from −92°C for PFW to an average value around −86°C for all iron oxide excess compositions (Fig. 7(b)).

The diffuseness of the transition decreases from about 75°C for PFW, to an average value of 52°C for the samples with iron oxide excess. Effectively the ferroelectric paraelectric phase transition becomes less diffuse for all these iron oxide excess compositions, which are then presenting the highest degree of homogeneity of all the studied compositions.

In contrast, the magnitudes of the dielectric

Table 3. Dielectric characteristics of PFW and PFW plus iron or lead oxide at 10, 50 and 100 kHz

Composition	*Frequency (kHz)*	E_{rmax}	E_r (20°C)	T_0°C	δ (°C)
PFW	10	6955	2963	−92·08	75·21
	50	6843	2963	−88·96	
	100	6791	2940	−87·34	
PFW2F	10	10440	3452	−86·08	53·76
	50	10131	3434	−82·18	
	100	9977	3428	−81·18	
PFW5F	10	12335	3831	−86·59	51·03
	50	11918	3818	−83·75	
	100	11696	3812	−82·77	
PFW10F	10	9104	2701	−86·7	52·41
	50	8849	2686	−84·36	
	100	8722	2681	−83·44	
PFW2P	10	4882	2553	−95·26	95·17
	50	4806	2534	−91·31	
	100	4769	2524	−89·35	
PFW5P	10	3770	2009	−99·22	108·49
	50	3665	1983	−92·32	
	100	3615	1965	−91·35	
PFW10P	10	2445	1361	−98·05	111·11
	50	2416	1352	−95·06	
	100	2404	1351	−91·07	

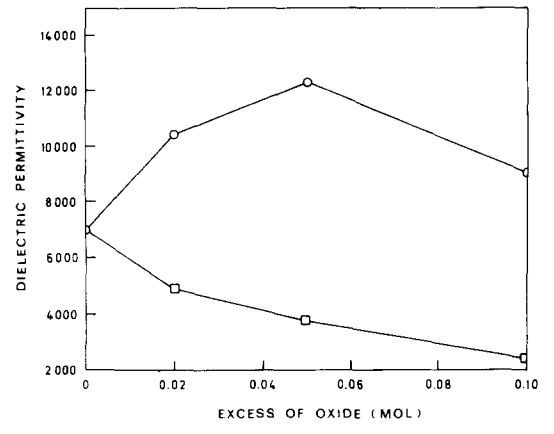

(a)

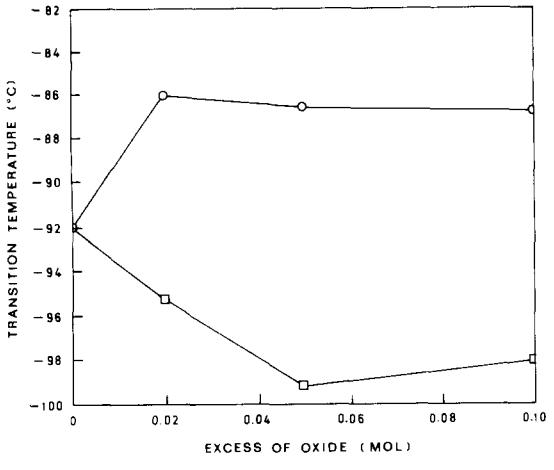

(b)

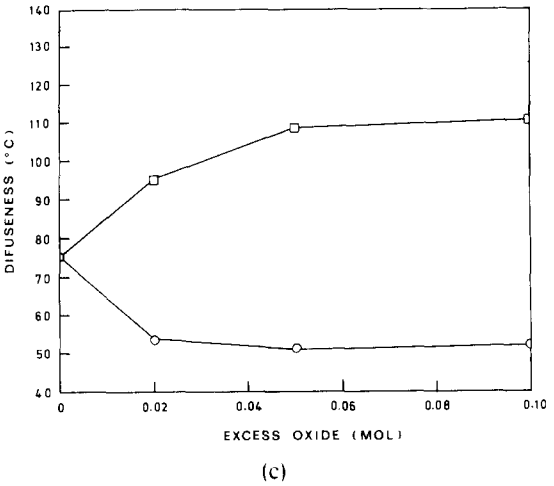

(c)

Fig. 7. The effect of excess (○) Fe_2O_3 and (□) PbO on (a) the maximum of the dielectric constant, (b) the transition temperature and (c) the diffuseness of PFW ceramics, at 10 kHz.

maxima steadily decrease for the samples with increasing excess of PbO (Fig. 7(a)). The transition range is shifted to lower temperatures together with a steady increase of the diffuseness (Fig. 7(b) and (c)).

The reason for the effects just described can be related to the Pb_2WO_5 phase present. Taking first the variations in the dielectric constant, it is evident that increasing amounts of a phase with a lower dielectric constant (E_r for $Pb_2WO_5 = 1190$) will decrease the dielectric constant of lead oxide excess compositions. Besides, these samples developed a more porous microstructure, unsuitable for attaining good dielectric characteristics. The same argument justifies the significant enhancement of the dielectric constant of samples with iron oxide excess up to 0·05 mol, since the amount of Pb_2WO_5 is decreasing in these samples. A monophasic material can be obtained when a proper addition of iron oxide excess is used. Above that value the dielectric constant of the diphasic material, now containing free Fe_2O_3, would decrease again, according to the rule of mixtures.

Turning now to the phase transitions temperature and diffuseness values presented in Table 3 and Fig. 7(b) and (c) it can be concluded that the PFW phase present in all the compositions, from where the Pb_2WO_5 phase has been eliminated (PFW5F and PFW10F), does not vary significantly, since the values of the phase transition ($T_0 = -86$ °C) and diffuseness ($\delta = 52$ °C) are approximately maintained. On the other hand, the regular change of the transition temperature to lower temperatures and the steady increase of the diffuseness of the transition for the four compositions containing increasing amounts of Pb_2WO_5 (PFW, PFW2P, PFW5P and PFW10P), indicate that changes were also occurring in the structure of the PFW phase, the only one responsible for the diffuse phase transition, since Pb_2WO_5, the other phase present, has no ferroelectric paraelectric phase transition in this temperature range.

As pointed out before, increasing amounts of PbO, in the excess lead oxide samples, gave increasing amounts of Pb_2WO_5 second phase (Table 2). The PFW phase formed under these circumstances has to be tungsten deficient or, in other words, must contain increasing amounts of tungsten vacancies in the B-site cation lattice. As the concentration of W^{6+} is decreasing it seems that the probability of getting Fe^{3+} and W^{6+} ions together in the right proportions to make an ordered B-site lattice is smaller, and as a result, an overall structure with a high degree of disorder will be formed. Excess amounts of Fe_2O_3, up to 0·02 mol, lead to a decrease of diffuseness to a value that was unaltered by using higher excess concentrations of Fe_2O_3. When a diphasic material containing Pb_2WO_5 is transformed into a monophasic material by Fe_2O_3 addition, the perovskite PFW then formed has to be Pb deficient, since the ratio Pb/W is 3:1 in the perovskite and 2:1 in the lead tungstate. It has been reported[38] that in other Pb-based relaxor systems, the presence of Pb vacancies was necessary to facilitate the exchange of B-site cations, when forming a more ordered state. The present results for the Fe_2O_3 excess compositions, the ones that present the highest degree of order, seem to confirm these

observations. If the models recently proposed for the relaxor behaviour[3,4,39–41] also apply to the PFW system, the described structural changes should correlate with changes in the micropolar regions giving polarization fluctuations. Work in progress using high-resolution TEM and frequency dependence of the dielectric maximum is trying to access the contribution of chemical lattice inhomogeneities or micropolar fluctuations to the relaxor behaviour of these PFW-type materials.

4 Conclusions

From the study of excess of lead oxide (0·02–0·10 mol) and iron oxide (0·02–0·10 mol) in $Pb(Fe_{2/3}W_{1/3})O_3$ it is possible to conclude that:

(1) Excess PbO decreases the amount of the perovskite phase, increasing the amount of the Pb_2WO_5 phase. Excess Fe_2O_3 increases the amount of the perovskite phase, due to the reaction with the Pb_2WO_5 phase. The dielectric constant was therefore increased, attaining values around 12500. Submicrometer iron-rich particles were detected for the 0·05 and 0·10 mol excess Fe_2O_3 compositions.

(2) Sintered samples with excess Fe_2O_3 present a high degree of densification, uniform microstructures and round-shaped grains. Sintered samples with excess of PbO present a poorer degree of densification, higher porosity and polyhedral shaped grains. The reason for these differences could be explained by CHR measurements.

(3) The excess PbO, giving a PFW phase deficient in tungsten, results in a more highly disordered structure. Probably the decreasing concentration of W^{6+} ions reduces the chances of Fe^{3+} and W^{6+} ions getting together to form an ordered B-site lattice.

(4) Excess iron oxide reacting with Pb_2WO_5 gives rise to a Pb-deficient PFW structure. A less diffuse phase transition, corresponding to a more ordered structure, is observed, in agreement with published results,[38] suggesting that A-site vacancies make the diffusion of the B-ions easier.

Acknowledgement

The authors wish to thank A. M. R. Senos for the assistance with dilatometric measurements and useful discussions.

References

1. Agranovskaya, A. I., Physical–chemical investigation of the formation of complex ferroelectrics with perovskite structure. *Bull. Acad. Sci. USSR, Phys. Ser.*, (1960) 1271–7.
2. Smolenski, G. A., Agranovskaya, A. I. & Isupov, V. A., New ferroelectrics of complex composition, III. Pb_2MgWO_6, $Pb_3Fe_2WO_9$, Pb_2FeTaO_6. *Sov. Phys. Sol. State*, **1** (1959) 907–8.
3. Viehland, D., Jang, S. J., Cross, L. E. & Wuttig, M., Freezing of the polarization fluctuations in lead magnesium niobate relaxors. *J. Appl. Phys.*, **68**(6) (1990) 2916–21.
4. Randall, C. A. & Bhalla, A. S., Nanostructural-property relations in complex lead perovskites. *Jap. J. Appl. Phys.*, **29**(2) (1990) 327–33.
5. Uchino, K. & Nomura, S., Crystallographic and dielectric properties in the solid solution systems $Pb(Fe_{2/3}W_{1/3})O_3$–$Pb(Mg_{1/3}Ta_{2/3})O_3$ and $Pb(MgW)_{1/2}O_3$–$Pb(FeTa)_{1/2}O_3$. *J. Phys. Soc. Jap.*, **41**(2) (1976) 542–7.
6. Uchino, K. & Nomura, S., Phenomenological theory of ferroelectricity in solid solution systems $Pb(Fe_{2/3}W_{1/3})O_3$–$Pb(M_{1/2}W_{1/2})O_3$ (M = Mn, Co, Ni). *Jap. J. Appl. Phys.*, **18**(8) (1979) 1493–7.
7. Jang, S. J., Schulze, W. A. & Biggers, J. V., Low-firing capacitor dielectrics in the system $Pb(Fe_{2/3}W_{1/3})O_3$–$Pb(Fe_{1/2}Nb_{1/2})O_3$–$Pb_5Ge_3O_{11}$. *Am. Ceram. Soc. Bull.*, **62**(12) (1983) 216–18.
8. Yonezawa, M., Low-firing multilayer capacitor materials. *Am. Ceram. Soc. Bull.*, **62**(12) (1983) 1375–83.
9. Shimada, Y., Utsumi, K., Yonezawa, M. & Takamizawa, H., Properties of large-capacitance multilayer ceramic capacitor. *Jap. J. Appl. Phys.*, **20**, Suppl. 20–4 (1981) 143–6.
10. Takamizawa, H., Utsumi, K., Yonezawa, M. & Ohno, T., Large capacitance multilayer ceramic capacitor. *IEEE, Trans. Com. Hybrids. Manuf. Techno., CHMT-4*, **4** (1981) 345–9.
11. Kassarjian, M. P., Newnham, R. E. & Biggers, J. V., Sequence of reactions during calcining of lead–iron-niobate dielectric ceramic. *Am. Ceram. Soc. Bull.*, **64**(8) (1985) 1108–11.
12. Kassarjian, M. P., Newnham, R. E. & Biggers, J. V., Reduction of losses in lead–iron-niobate dielectric ceramics. *Am. Ceram. Soc. Bull.*, **64**(9) (1985) 1245–8.
13. Yonezawa, M., Utsumi, K. & Ohno T., Properties of the multilayer capacitor $Pb(Zn_{1/3}Nb_{2/3})O_3$–$Pb(Fe_{1/2}Nb_{1/2})O_3$–$Pb(Fe_{2/3}W_{1/3})O_3$ ternary system. In *Proceedings of the 2nd Meeting on Ferroelectric Materials and their Applications*, F-4, 1979, pp. 215–20.
14. Iizawa, O., Fujiwara, S., Ueoka, H., Furukawa, K., Kikuchi, N. & Tanaka, H., High dielectric constant type ceramic composition. US Patent, 4 235 635, 1984.
15. Yonezawa, M. & Ohno, T., Ceramic compositions having high dielectric constant. US Patent 4 236 928, 1980.
16. Ouchi, H. & Matsua, Y., High permittivity ceramic compositions. Japanese Patent 59 54665, 1984.
17. Lejeune, M. & Boilot, J. P., Formation mechanism and ceramic process of the ferroelectric perovskites: $Pb(Mg_{1/3}Nb_{2/3})O_3$ and $Pb(Fe_{1/2}Nb_{1/2})O_3$. *Ceram. Int.*, **8**(3) (1982) 89–103.
18. Lejeune, M. & Boilot, J. P., Optimization of dielectric properties of lead–magnesium niobate ceramics. *Am. Ceram. Soc. Bull.*, **64**(4) (1986) 679–82.
19. Swartz, S. L. & Shrout, T. R., Fabrication of perovskite lead magnesium niobate. *Mat. Res. Bull.*, **17** (1982) 1245–50.
20. Groves, P., Fabrication and characterization of ferroelectric perovskite lead indium niobate. *Ferroelectrics*, **65**(1/2) (1985) 67–77.
21. Furukawa, K., Fujiwara, S. & Ogasawara, T., Dielectric properties of $Pb(Mg_{1/3}Nb_{2/3})O_3$–$PbTiO_3$ ceramics for capacitor materials. In *Proceedings of the Japan–US Study Seminar on Dielectric and Piezoelectric Ceramics*, P.T.-4, 1982, pp. 1–5.
22. Swartz, S. L., Shrout, T. R., Schulze, W. A. & Cross, L. E.,

Dielectric properties of lead–magnesium niobate ceramics. *J. Am. Ceram. Soc.*, **67**(5) (1984) 311–15.
23. Goo, E., Yamamoto, T. & Okazaki, K., Microstructure of lead–magnesium niobate ceramics. *J. Am. Ceram. Soc.*, **68**(8) (1986) C188–C189.
24. Wang, H. C. & Schulze, W. A., The role of excess magnesium oxide or lead oxide in determining the microstructure and properties of lead magnesium niobate. *J. Am. Ceram. Soc.*, **73**(4) (1990) 825–32.
25. Kang, D. H. & Yoon, K. H., Dielectric properties due to excess and MgO in lead magnesium niobate ceramics. *Ferroelectrics*, **87** (1988) 255–64.
26. Guha, J. P., Hong, D. J. & Anderson, H. U., Effect of excess PbO on the sintering characteristics and dielectric properties of $Pb(Mg_{1/3}Nb_{2/3})O_3$–$PbTiO_3$ based ceramics. *J. Am. Ceram. Soc.*, **71**(3) (1988) C152–C154.
27. Chen, J., Gorton, A., Chan, H. M. & Harmer, M. P., Effect of power purity and second phases on the dielectric properties of lead magnesium niobate ceramics. *J. Am. Ceram. Soc.*, **69**(12) (1986) C303–C305.
28. Yasuda, N., Fujimoto, S. & Tanaka, K., Dielectric properties of $Pb(Fe_{2/3}W_{1/3})O_3$ under pressure. *J. Phys.: D. Appl. Phys.*, **18** (1985) 1909–17.
29. Yonezawa, M. & Ohno, T., Perovskite formation process and properties of the system $Pb(Fe_{2/3}W_{1/3})O_3$. In *Proceedings of the Japan–US Study Seminar on Dielectric and Piezoelectric Ceramics*, T-8, 1982, pp. 1–5.
30. Lu, C. H., Shinozaki, K., Mizutani, N. & Kato, M., Liquid-phase formation in reaction process of $3PbO.Fe_2O_3.WO_3$. *Seramikkusu Ronbunshi*, **97**(2) (1989) 119–24.
31. Lu, C. H., Ishizawa, N., Shinozaki, K., Mizutani, N. & Kato, M., Synthesis and cell refinement of $Pb(Fe_{2/3}W_{1/3})O_3$ and pyrochlore-related phase in the Pb–Fe–W–O system. *J. Mat. Sci. Lett.*, **7** (1988) 1078–9.
32. Lu, C. H., Shinozaki, K., Kato, M. & Mizutani, N., Preparation and thermal decomposition of new pyrochlore $Pb_2FeWO_{6.5}$. *J. Mat. Sci.*, **26** (1991) 1009–14.
33. Vilarinho, P. M., Senos, A. M. R. & Baptista, J. L., Synthesis, sintering and dielectric characterization of lead tungstate perovskite ceramics. In *Proceedings of the 7th CIMTEC World Ceramic Congress, Materials Monographs*, 66C, ed. P. Vicenzini. Elsevier, 1991, pp. 2047–56.
34. Huppman, W. J. & Riegger, H., Modelling of rearrangement processes in liquid phase sintering. *Acta Met.*, **23**(8) (1975) 965–9.
35. Yang, W. F. & Cutler, I. B., Initial sintering with constant rate of heating. *J. Am. Ceram. Soc.*, **53**(42) (1970) 659–63.
36. Senos, A. M. R., Santos, M. R. A. & Vieira, J. M., Effects of practical morphology and rearrangement on sintering of ZnO fine powders. In *Science of Ceramics 14*, ed. D. Taylor. Butler and Tamer Ltd, London, 1988, pp. 255–71.
37. Pilgrim, S. R., Sutherland, A. E. & Winzer, S. R., Diffuseness as a useful parameter for relaxor ceramics. *J. Am. Ceram. Soc.*, **73**(10) (1990) 3122–5.
38. Wang, H. C. & Schultz, W. A., Order–disorder phenomenon in lead scandium tantalate. *J. Am. Ceram. Soc.*, **73**(5) (1990) 1228–34.
39. Viehland, D., Jang, S. J., Cross, L. E. & Wuttig, M., Local polar configuration in lead magnesium niobate relaxors. *J. Appl. Phys.*, **69**(1) (1991) 414–19.
40. Viehland, D., Jang, S. J., Cross, L. E. & Wuttig, M., The dielectric relaxation of lead magnesium niobate relaxor ferroelectrics. *Phil. Mag. B*, **64**(3) (1991) 335–40.
41. Viehland, D., Li, J. F., Jang, S. J., Cross, L. E. & Wuttig, M., Dipolar glass model for lead magnesium niobate. *Phys. Rev. B.*, **43**(10) (1991) 8316–21.